INSTITUTE FOR FUSION STUDIES

DOE/ET-53088-453 IFSR #453

Drift Wave Vortices in Inhomogeneous Plasmas

X.N. Su, W. Horton, and P.J. Morrison
Institute for Fusion Studies
The University of Texas at Austin
Austin, Texas 78712

August 1990

THE UNIVERSITY OF TEXAS

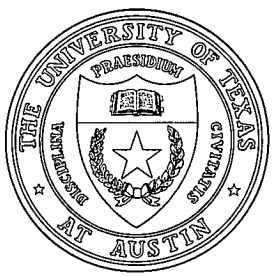

AUSTIN

Drift Wave Vortices in Inhomogeneous Plasmas

X.N. Su, W. Horton, P.J. Morrison
Department of Physics and Institute for Fusion Studies
The University of Texas at Austin
Austin, Texas 78712

Abstract

The effects of density and temperature gradients on drift wave vortex dynamics are studied using a fully nonlinear model with the Boltzmann density distribution. The equation based on the full Boltzmann relation, in the short wavelength ($\sim \rho_s$) region possesses no localized monopole solution, while in the longer wavelength ($\sim (\rho_s r_n)^{1/2}$) region the density profile governs the existence of monopole-like solutions. In the longer wavelength regime, however, the results of analysis show that due to the inhomogeneity of the plasma the monopoles cannot be localized sufficiently to avoid coupling to propagating drift waves. Thus, the monopole drift wave vortex is a long lived coherent structure, but it is not precisely a stationary structure since the coupling results in a "flapping" tail. The flapping tail causes energy of the vortex leaking out, but the effect of the temperature gradient is to reduce the leaking of this energy.

I. Introduction

It is well known that the dipole vortex is an exact solitary wave solution to the dissipationless Hasegawa-Mima[1] (H-M) drift wave equation, which in the fluid mechanics literature is referred to as the Rossby wave equation

$$(1-\nabla^2)\frac{\partial\varphi}{\partial t}+v_d\frac{\partial\varphi}{\partial y}-[\varphi,\nabla^2\varphi]=0 \tag{1}$$

where

$$[\varphi,\nabla^2\varphi]=\frac{\partial\varphi}{\partial x}\frac{\partial\nabla^2\varphi}{\partial y}-\frac{\partial\varphi}{\partial y}\frac{\partial\nabla^2\varphi}{\partial x}$$

is the Jacobian between the electrostatic potential φ and the vorticity $\zeta=\nabla^2\varphi$. The convective nonlinearity $[\varphi,\zeta]$ of Eq. (1), also known as the Poisson-bracket or vector nonlinearity, facilitates the formation of dipole vortices.[2,3] Recently, there have been numerous studies of this type of nonlinearity and the resulting vortex dynamics.[3,4] In the present work, we consider a generalization of the H-M drift wave equation that includes a general density profile $n_0(x)$ and temperature profile $T_e(x)$[5-11].

Petviashvili[5] first studied the problem with a temperature gradient and an exponential density profile. The model he proposed has recently been criticized by several authors[7-11] because of inconsistency with Ertel's theorem, the basic conservation law of potential vorticity. Some of these authors[7,8] showed that monopole vortices exist only when the drift velocity in Eq. (1) is nonconstant, $v_d=v_d(x)$. More recently, Spatschek *et al.*[12] used a new high order and long wavelength scaling to develop a model that is similar to Petviashvili's model. These authors argue for the existence of a monopole vortex solution in very long wavelength region ($\sim\rho_s/\epsilon$) even with constant drift velocity v_d. Here ϵ is the usual drift theory expansion parameter $\epsilon=\rho_s/r_n$ where $\rho_s=c(m_iT_e)^{1/2}/eB$ is drift wave dispersion scale length and r_n is the density gradient scale length. We also define $\eta_e=r_n/r_{T_e}$ as the ratio of the density-to-temperature gradient scale length.

It is well known that there exists a large class of vortex solutions for nonlinear drift waves. These solutions arise because of an arbitrary function $F(\varphi - ux)$ that appears in the equation for travelling wave solutions. Usually this function is chosen such that the solution converges to zero as $r \rightarrow \infty$. The function F determines the relationship between the generalized potential vorticity, which to the first order is $\nabla^2\varphi - \varphi/T(x) - \ell n\, n_0(x)$, and the stream function, $\varphi - ux$, in a frame traveling with speed u. For the well known dipole vortex solution, the choice of this relationship is a piece-wise linear with a jump in the slope $dF/d\varphi$. In spite of the presense of this jump the solution is consistent with the H-M equation[3,10]. Alternatively one can demand F to be analytic. In this work we show for the model that includes both temperature and density gradients when the density gradient is constant, this choice of F makes it impossible to have a binding effective potential for the case of a strictly exponential density profile. This result is independent of the temperature profile. However, with a more complex background plasma; i.e. with nonconstant drift wave velocity $v_d(x)$, the monopole vortex is found in the $\rho_s/\epsilon^{1/2}$ wavelength region. Physically the nonconstant $v_d(x)$ adds a shear to the diamagnetic drift velocity. Since it is well known (Horton *et al.*[13] and Sagdeev *et al.*[14]) that shear flow causes the formation of monopole vortices, it is perhaps to be expected that the shear flow from nonuniform $v_d(x)$ will create monopole solitary waves.

Also we show that the monopole vortices mentioned above in inhomogenuous plasmas are not strictly localized soliton-like monopoles. The effect of inhomogeneity in the background plasma on vortex dynamics is shown to give arise to a oscillating tail; the inhomogeneity forces a coupling of the vortex core to the tail of a radiative wake of drift waves which thus causes radiative damping of the vortex core.

This work is organized as follows: in Sec. II, we derive the model equation for nonlinear drift waves in plasmas with density and temperature gradients. the steady state travelling wave equation of the model is given and solutions of this equation are discussed in Sec. III.

In Sec.IV we investigate the effect of inhomogeneity in the drift wave vortex and give analytical results. Section V describes the results of numerical investigation. Summary and the conclusions are given in Sec. VI.

II. Model Equation

We consider a plasma in a uniform external magnetic field in the z-direction, where the electrons move freely along the magnetic field. The dissipationless equation of motion and continuity equation for the ions are

$$\frac{d\mathbf{v}}{dt} = -\frac{e}{m_i}\nabla\Phi + \omega_{ci}\mathbf{v}\times\hat{\mathbf{z}} \tag{2}$$

$$\frac{\partial n}{\partial t} + \nabla\cdot(n\mathbf{v}) = 0\,, \tag{3}$$

where $d/dt = \partial/\partial t + \mathbf{v}\cdot\nabla$ and $\omega_{ci} = eB/m_i c$ is the ion cyclotron frequency. Combining these two equations, one can easily derive the Ertel's theorem by neglecting the parallel compression $\nabla_{\|}v_{\|}$,

$$\frac{d}{dt}\left(\frac{\omega_{ci}+\omega_z}{n}\right) = 0 \tag{4}$$

where $\omega_z = \hat{\mathbf{z}}\cdot(\nabla\times\mathbf{v})$.

With the ordering,

$$\epsilon_t \equiv \frac{1}{\omega_{ci}}\frac{\partial}{\partial t} \sim \frac{\mathbf{v}\cdot\nabla}{\omega_{ci}} \ll 1\,,$$

to the lowest order in ϵ_t, we have

$$\mathbf{v} = (\frac{e}{m_i\omega_{ci}})\hat{\mathbf{z}}\times\nabla\Phi\,,$$

$$\omega_z = \omega_{ci}\frac{\rho_s^2}{T_e}\nabla^2(e\Phi)\,,$$

and

$$\frac{d}{dt} = \frac{\partial}{\partial t} + \omega_{ci}\frac{\rho_s^2}{T_e}[e\Phi\,,\,]$$

where $\rho_s = c_s/\omega_{ci}$ and $c_s = (T_e(x)/m_i)^{1/2}$. Now we define $T(x) = T_e(x)/T_0$ (where T_0 is a constant), $\varphi = (r_n/\rho_{s0})e\Phi/T_0$, and $\epsilon_n = \rho_{s0}/r_n$. Eq. (4) becomes

$$\frac{\partial}{\partial t}\left(\frac{1+\epsilon_n\nabla^2\varphi}{n}\right) + \left[\varphi, \quad \frac{1+\epsilon_n\nabla^2\varphi}{n}\right] = 0\,. \tag{5}$$

Here the space and time variables are normalized by ρ_{s0} and r_n/c_{s0}, respectively, $r_n^{-1} = -d\ell n\, n_0/dx$, ρ_{s0} and c_{s0} are the ion Larmor radius and ion acoustic speed at the reference electron temperature T_0, respectively. Equation (5) states that the potential vorticity is conserved on each fluid element following the velocity $\mathbf{v} = \hat{\mathbf{z}} \times \nabla\varphi(x,y,t)$.

To close Eq. (5), we assume that the particles satisfy the condition of qusi-neutrality with the electrons obeying the Boltzmann density distribution. Thus, the ion density is given by

$$n = n_0(x)exp[\frac{e\Phi}{T_e(x)}] = n_0(x)exp[\frac{\epsilon_n\varphi}{T(x)}]\,, \tag{6}$$

where $n_0(x)$ and $T(x)$ are assumed to be analytic functions. Due to the fact that ϵ_n is a small parameter, for the numerical calculations in Sec. V the exponential in Eq. (6) is expanded to first order in ϵ_n. For certain strong monopole solutions with large negative φ, however, the expansion can lead to negative density state[6]. Thus, whenever the expansion is performed we require that $\epsilon_n\varphi < T$ for all x.

III. Travelling Wave Equation and Solutions

Now we look for travelling stationary wave solutions of Eq. (5) of the form $\varphi = \varphi(x, y-ut)$. Such solutions travel with the velocity u in the y-direction. Equation (5) and (6) together give the following:

$$-u\frac{\partial G}{\partial y} + [\varphi\,,\, G] = 0 \tag{7}$$

where

$$G = \frac{1+\epsilon_n\nabla^2\varphi}{n_0(x)exp(\epsilon_n\varphi/T(x)}\,.$$

Equation (7) gives the condition for stationarity as

$$[\varphi - ux\,,\, G] = 0\,, \tag{8}$$

which requires that

$$\frac{1+\epsilon_n\nabla^2\varphi}{n_0(x)exp\,(\epsilon_n\varphi/T(x))} = F(\varphi - ux) \tag{9}$$

where F is an arbitrary function of its argument.

If we follow Ref. (7) and choose F to be an analytic function determined by $n_0(x)$, then Eq. (9) becomes

$$\epsilon_n\nabla^2\varphi = \frac{n_0(x)}{n_0(x-\frac{\varphi}{u})}exp(\frac{\epsilon_n\varphi}{T(x)}) - 1\,, \tag{10}$$

where

$$F(\varphi - ux) = \frac{1}{n_0\left(\frac{ux-\varphi}{u}\right)}\,. \tag{11}$$

With this choice of F the right hand side of Eq. (10) approaches to zero as $|x| \to \infty$ and $\varphi \to 0$, which corresponds to the untrapped flow region. Although there exist other analytic choices for F that satisfy $\nabla^2\varphi \to 0$ as $|x| \to \infty$ and $\varphi \to 0$ which may lead to localized solutions for reasonable density profiles $n_0(x)$, for the strictly exponential profile $n_0(x) = exp(-\epsilon_n x)$ and the F of Eq. (11), bound solutions do not exist. In this case Eq. (10) becomes the following nonlinear Poisson equation for φ:

$$\epsilon_n\nabla^2\varphi = exp\left[\epsilon_n(\frac{1}{T(x)} - \frac{1}{u})\varphi\right] - 1 = -\frac{\partial}{\partial\varphi}\left[\varphi - \frac{exp\,[\epsilon_n(1/T(x) - 1/u)\varphi]}{\epsilon_n(1/T(x) - 1/u)}\right] \tag{12}$$

The effective potential for Eq. (12) is then

$$V_{exp}(\varphi, x) = \varphi - \frac{exp\,[\epsilon_n(1/T(x) - 1/u)\varphi]}{\epsilon_n(1/T(x) - 1/u)}. \tag{13}$$

We can easily see that this effective ("time" dependent) potential $V_{exp}(\varphi, x)$ for any temperature profile $T(x)$, is simply not able to form a soliton well, and thus bind a local disturbance to form a solitary vortex (monopole or dipole). However, the fact that this choice for F does

not produce a localized solution does not exclude the possibility that the dynamics of the the plasma in relaxaing from a turbulent state finds another choice of $F(\varphi - ux)$ with a new structure that allows binding.

Since trapping, like scooping ice cream, is an inherently nonanalytic process, it is natural to follow the modon construction for the dipole vortex and choose $F(\varphi - ux)$ to be piecewise smooth. For the dipole vortex, F is the same as Eq.(11) for the untrapped region $r > r_0$ and a different interior function $F_{int}(\varphi - ux)$ with opposite signed slope $dF/d\varphi$ for $r < r_0$. To see the relationship with the dipole vortex solution we consider the logarithm of Eq. (9)

$$\ell n\,(1 + \epsilon_n \nabla^2 \varphi) = \ell n\, F(\varphi - ux) + \ell n\, n_0 + \frac{\epsilon_n \varphi}{T(x)}. \tag{14}$$

With $n_0(x) = exp(-\epsilon_n x)$, $F(\varphi - ux) = exp[\epsilon_n(x - \varphi/u)]$ as defined by Eq. (11) and ordering

$$u \sim v_{d0} = 1\,, \qquad \frac{e\Phi}{T_e} \sim \frac{\rho_{s0}}{r_{n0}} \equiv \epsilon_n \sim \epsilon \ll 1\,, \tag{15}$$

by keeping the lowest order in ϵ we obtain, from Eq.(14),

$$\nabla^2 \varphi = \left(\frac{1}{T(x)} - \frac{v_{d0}}{u}\right)\varphi \qquad for \qquad r \geq r_0\,. \tag{16}$$

For the interior ($r < r_0$) solution we choose

$$\ell n\, F_{int}(\varphi - ux) = -\epsilon_n(1 + p^2)(\varphi - ux)\,, \tag{17}$$

so that, to the lowest order in ϵ, Eq. (14) reduces to

$$\nabla^2 \varphi + \left(1 + p^2 - \frac{1}{T(x)}\right)\varphi = \left[u(1 + p^2) - 1\right] x \qquad for \qquad r < r_0\,. \tag{18}$$

Eq. (18) for the interior vortex structure is driven by source term which measures the mismatch between the vortex speed u and the linear wave speed $1/(1+p^2)$. The constant $p^2 > 0$ is determined by continuity of φ, $\partial\varphi/\partial r$, and $\nabla^2\varphi$ at $r = r_0$. In the case where $T = constant$ this choice for $F(\varphi - ux)$ produces dipole solutions[3] of radius r_0 with an amplitude that increases as $v_{d0} r_0$. Thus, while we can show that the simplest, analytic choice of $F(\varphi - ux)$

forbids the existence of monopole vortices for the strictly exponential density profile, the plasma dynamics in relaxing from a turbulent state in which trapping takes place may naturally produce nonanalytic $F(\varphi - ux)$ at the point of transition from trapping to untrapping flows. An example from turbulent particle simulation that demostrates the change in the slope of $F(\varphi - ux)$ as plotted versus vorticity is shown in Horton *et al.*(1987)[13]. However, the dipole vortices have been shown[6,12] to be structurely unstable, in particularly, a small term of KdV nonlinearity can split them into monopole-like vortices, into which we now turn.

In most magnetic confinement systems both $T_e(x)$ and $v_d(x)$ vary on the scale of r_n. We define the dimensionless parameters $\kappa_T \equiv \rho_{s0} d(1/T)/dx \sim \epsilon$ and $v'_{d0} \equiv \rho_{s0} dv_d/dx \sim \epsilon_n v_{d0}$. In the case of a nonconstant drift velocity $v_d(x)$, with or without a temperature gradient, the analytic choice of $F(\varphi - ux)$ in Eq. (11) can lead to the possibility of trapping to form solitary vortices. Taking the logarithm of Eq. (10)

$$\ell n(1 + \epsilon_n \nabla^2 \varphi) = \ell n\, n_0(x) - \ell n\, n_0(x - \frac{\varphi}{u}) + \frac{\epsilon_n \varphi}{T(x)}\,. \tag{19}$$

and expanding the density profile as

$$\ell n\, n_0(x) = -\epsilon_n (v_{d0} x + \frac{v'_{d0}}{2} x^2 + ...) \tag{20}$$

yields

$$\ell n(1 + \epsilon_n \nabla^2 \varphi) = \epsilon_n k^2(u, x)\varphi + \epsilon_n \frac{v'_{d0}}{2u^2} \varphi^2 + \ ... \tag{21}$$

where

$$k^2(u, x) \equiv \frac{1}{T(x)} - \frac{v_d(x)}{u} \tag{22}$$

and

$$v_d(x) = 1 + v'_{d0} x\,. \tag{23}$$

Observe that $v_{d0} = 1$ follows from the choice of space time units.

With the ordering

$$\rho_{s0}^2\nabla^2 \sim \frac{e\Phi}{T_e} \sim \kappa_T \sim v'_{d0} \sim \frac{\rho_{s0}}{r_{n0}} \equiv \epsilon_n \sim \epsilon \ll 1\,, \quad and \quad u \sim v_{d0} = 1 \tag{24}$$

and keeping only the terms of order ϵ^2 in Eq. (21), we get

$$\nabla^2\varphi = k_0^2\varphi + \frac{v'_{d0}}{2u^2}\varphi^2 \tag{25}$$

where we have expanded $k^2(u,x) = k_0^2 + \alpha x + \ldots$ and considered $k_0^2 = (1 - v_{d0}/u) \sim \epsilon$ and $\alpha = (\kappa_T - v'_{d0}/u) \sim \epsilon^2$.

We notice that Eq. (25) has the same form as the Petviashvili equation for the steady state[5]. But the crucial difference is that in Petviashvili equation the nonlinear term arises due to the temperature gradient, while in the present case, the nonlinear term is caused by the gradient of drift velocity. However, the gradient of the drift velocity also gives rise to a linear damping term $-(v'_{d0}/u)x\varphi$ on the right side of Eq. (25) which has the same order as the other terms. The important thing is that although the temperature gradient does not contribute to nonlinear term, its existence can balance the linear damping term caused by the gradient of drift velocity v'_{d0}. In this way the linear damping term is made smaller and exact monopole vortex solutions are possible when $\kappa_T = v'_{d0}/u$ or $\alpha = 0$.

The quadratic nonlinear Poisson Eq. (25) has monopole vortex solutions[6,8] when $k_0^2 \equiv (1/T - v_d/u)_0 > 0$. The solutions can be approximately[8,15] written as the following, for small r,

$$\varphi(x,y,t) = -2.4k_0^2(\frac{2u^2}{v'_{d0}})\left[cosh\left(\frac{3}{4}k_0\sqrt{x^2+(y-ut)^2}\right)\right]^{-\frac{4}{3}}\,. \tag{26}$$

From Eq. (25) and Eq. (26) we can see that the sign of the vortex amplitude no longer depends on the sign of velocity u as is the case for Petviashvili monopoles. Instead it depends on the sign of v'_{d0}. From Eq. (25), we recognize the symmetry relation

$$\varphi(-v'_{d0};x,y) = -\varphi(v'_{d0};x,y),$$

a relation we test in the simulation shown in Fig. (1). The simlation shows that if we initialize with the dipole vortex (solution of the H-M equation), the dipole will first separate into two monopoles, cyclone $\varphi < 0$ and anticyclone $\varphi > 0$, which was first reported by Su *et al.*[6] (1988). Finally, only one monopole survives. Which monopole survives is determined by the sign of v'_{d0}. If $v'_{d0} > 0$, only the cyclone survives, while if $v'_{d0} < 0$, only the anticyclone survives.

We have also tested the new monopole vortex solution given here for soliton-like behavior upon collision. Preliminary results show that the overtaking collision is largely elastic. Details of these studies will be reported in a subsequent work.

The following amplitude-velocity relation can be obtained from Eq. (26):

$$u = \frac{v_{d0} \pm \sqrt{v_{d0} + 0.83|v'_{d0}\varphi_m|}}{2} \tag{27}$$

where φ_m is the amplitude of the monopole vortex given by Eq. (26). However, the monopole vortex solutions given here must propagate in the direction of the drift wave ($u > 0$) since the negative velocity monopoles have $k_0^2 = 1 + v_{d0}/|u| \geq 1$, which violates the ordering in Eq. (24) required for localization. In this short wavelength region, $r_0 \sim \rho_{s0}$, there are no localized monopole solutions as discussed in Sec.II. Therefore we can only take positive sign in Eq. (27).

We can use the amplitude φ_m to estimate the maximum or minimum density of the vortex

$$n/n_0 = exp(\frac{\epsilon_n \varphi}{T(x)}) \approx exp(\epsilon_n \varphi_m) = exp\left(-\frac{4.8\epsilon_n}{v'_{d0}} u(u - v_{d0})\right) . \tag{28}$$

Deriving Eq. (25), and therefore Eq. (26) from Eq. (21) implies that we have expanded the Boltzmann density distribution of Eq. (6) to first order in ϵ_n and dropped all the higher order terms. For consistency of the expansion, there should be

$$\epsilon_n |\varphi_m| = \frac{4.8\epsilon_n}{|v'_{d0}|} u(u - v_{d0}) \leq 1$$

We therefore get the interval condition for the velocity u

$$v_{d0} \leq u \leq \frac{v_{d0} + \sqrt{v_{d0}^2 + 0.83|v'_{d0}|/\epsilon_n)}}{2} \tag{29}$$

required for the validity of the expansion. Eq. (29) shows that u must be the same order as v_{d0}. This implies that we consider $v'_{d0} \sim \epsilon_n$.

Using a multiple-scale method and a different ordering, namely taking

$$\rho_s^2 \nabla^2 \sim \frac{e\Phi}{T_e} \sim \frac{u}{c_s} \sim \kappa_T \sim k_0^2 \sim \epsilon^2 \,, \quad and \quad \frac{1}{\omega_{ci}} \frac{\partial}{\partial t} \sim \epsilon^5 \,, \tag{30}$$

Spatschek *et al.*[12] develop a model in which the steady state equation has a form similar to Eq. (25), but with a coefficient of the last nonlinear term in Eq. (25) proportional to $\kappa_T \equiv -(1/T)(\partial \ell n\, T/\partial x)$. Although both the equations, our Eq. (25) and Eq. (5) in Ref. (11) have been shown to have monopole solutions[5,6,12,15], in reality the vortex wave function will extend into the region where

$$k^2(u,x) = k_0^2 + \alpha x + ... < 0 \,. \tag{31}$$

When this happens outgoing drift wave propagation occours. The matching analysis in the following section shows that the amplitude of the outgoing wave is of order $\varphi_{vortex}(x = x_{crit})$ where x_{crit} is the point at which $k^2(u, x_{crit}) = 1/T - v_d/u = 0$. For large scale vortices with core size $r_0 \sim k_0^{-1} > \rho_{s0}/\epsilon^{2/3}$, in inhomogeneous plasma, the coupling to outgoing drift waves is a strong effect that eliminates the existence of the monopole vortex.

IV. Radiation Damping of Solitary Drift Wave Vortex in Inhomogeneous Plasmas

In the small amplitude region exterior to the vortex core the wave field is given, from Eq. (21), by

$$\frac{\partial^2 \varphi_{k_y}(x)}{\partial x^2} + \left[-(\frac{1}{T(x)} - \frac{v_d(x)}{u}) - k_y^2 \right] \varphi_{k_y}(x) = 0 \,, \tag{32}$$

with $\varphi_{k_y}(x)$ the Fourier transform in y of $\varphi(x,y,t)$ such that

$$\varphi(x,y,t) = \int dk_y \varphi_{k_y}(x) e^{ik_y(y-ut)} \ .$$

Equation (32) has turning points at $x = x_T$ where the x_T are determined by $v_d(x_T)/u - k_y^2 - 1/T(x_T) = 0$. For $k_y^2 \to 0$ the $x_T(k_y) \to x_{crit}$ defined by $k^2(u, x_{crit}) = 0$ in Eq. (31).

For $|x| > x_0$ in the exterior region, where x_0 is the length scale of vortex core given by $k_0 x_0 \simeq 1$, the WKB solutions of Eq. (32) are

$$\varphi_{k_y}(x) = \begin{cases} A_{k_y} Q_{k_y}^{-1/4}(x,u) \exp\left(i \int_{x_T}^{x} Q_{k_y}^{1/2}(x',u)dx'\right) , & Q_{k_y}(x,u) > 0 \\ A_{k_y}(-Q_{k_y}(x,u))^{-1/4} \exp\left(-\int_{x_T}^{x} (-Q_{k_y}(x',u))^{1/2} dx' - \frac{i\pi}{4}\right) , & Q_{k_y}(x,u) < 0 \end{cases} \tag{33}$$

where $Q_{k_y}(x,u) = v_d(x)/u - 1/T(x) - k_y^2$ and the amplitude A_{k_y} will be determined by matching to the vortex solution. Equation (33) with $Q_{k_y} > 0$ describes the outgoing radiation wave in the high density gradient and high temperature region. In the region where $v_d(x)/u - 1/T(x) < k_y^2$, we again expand $v_d(x)/u - 1/T(x) \simeq -k_0^2 - \alpha x > 0$. Then $x_T \simeq -(k_0^2 + k_y^2)/\alpha$ for $k_0^2 > 0$ and

$$\int_{x_T}^{x} (-Q_{k_y}(x,u))^{1/2} dx' \simeq [x - (2/3|\alpha|)(k_0^2 + k_y^2)](k_0^2 + k_y^2)^{1/2} \qquad for \quad |x_0| << |x| << |x_T| \, .$$

The approximate exterior vortex solution can be obtained by neglecting the nonlinear term in Eq. (25),

$$\varphi(x,y,t) \simeq \varphi_m K_0(k_0 r) \tag{34}$$

where $r = [x^2 + (y - ut)^2]^{1/2}$ and $\varphi_m = -4.8 k_0^2 u^2 / v'_{d0}$ is the amplitude of the vortex. The Fourier transform of Eq. (34) in y is[16]

$$\varphi_{k_y}(x) = \frac{\varphi_m}{2} \frac{exp(-|x|\sqrt{k_0^2 + k_y^2})}{\sqrt{k_0^2 + k_y^2}} \tag{35}$$

Matching Eq. (35) with Eq. (33) with $Q_{k_y} < 0$, we can obtain the radiation amplitude formula

$$A_{k_y} \simeq \frac{\varphi_m}{2(k_0^2 + k_y^2)^{1/4}} exp\left(i\frac{\pi}{4} - \frac{2}{3|\alpha|}(k_0^2 + k_y^2)^{3/2}\right) , \tag{36}$$

which is to be used in Eqs. (33). Therefore the monopole vortex solution of Eq. (25) is coupled to a radiation wave with significant amlitude unless the condition $|\alpha| << 2k_0^3/3 \sim \epsilon^{3/2}$ is satisfied.

We point out that in the case discussed in Ref. (11), where the type of the stationary equation is similar to that of Eq. (25) but with the longer wavelength scaling $k_0 \sim \epsilon$ and $\alpha \sim \epsilon^3$, the monopole vortices studied by Spatschek *et al.*[12] should have osillating tails with the substantial amplitude $\sim ((2/\epsilon)^{1/2}\varphi_m/4)exp(-2/3)$ as seen from Eq. (36). The numerical solutions given in their work do not show the oscillationg tail since their equation (Eq. (8) in Ref. (11)) does not explicitly contain the inhomogeneity. Their numerical results, therefore, are only for the very special case of $\kappa_T = v'_{d0}/u$, i.e., $\alpha = 0$. In this way the solutions which the authors give are essentially those given earlier by Su *et al.*[6] for the Petviashvili's equation.

The decay rate of energy of the solitary drift wave can be computed by using the energy conservation law,

$$\frac{\partial \mathcal{E}}{\partial t} + \nabla \cdot \mathbf{S} = 0\,, \tag{37}$$

where

$$\mathcal{E}(x,y,t) = \frac{1}{2}\left[\frac{\varphi^2}{T(x)} + (\nabla\varphi)^2\right]\,, \tag{38}$$

and

$$\mathbf{S} = \left(\frac{v_d(x)}{2}\varphi^2 - \frac{\kappa_T}{3}\varphi^3\right)\hat{\mathbf{y}} - \varphi\nabla\frac{\partial\varphi}{\partial t} - \nabla^2\varphi\left(\hat{\mathbf{z}}\times\nabla\frac{\varphi^2}{2}\right) \tag{39}$$

are the local energy density and the energy flux, respectively. Integrating Eq. (38) over the space volume, with the help of Eqs. (25), (26) and (34), we obtain the energy for the monopole vortex

$$E_v = \int \mathcal{E} d^3x \approx \frac{8.2\pi L_c u^4 k_0^2}{(v'_{d0})^2}(\frac{4}{3} + k_0^2) \tag{40}$$

where L_c is the length scale in z of the coherent vortex structure.

The outgoing wave propagation given by the matching of Eq. (35) to Eq. (33), leads to the decay of the vortex energy E_v. Integrating the energy balance Eq. (37) over the space volume $\int d^3x$, neglecting the last term of Eq. (39) proportional to φ^3 since φ is exponential small for $x >> x_0$, and using Parseval's theorem and Eq. (33) to evaluate the outgoing wave energy flux, gives the decay rate of vortex energy

$$\begin{aligned}
\frac{dE_v}{dt} &= \int d^3x \frac{\partial \mathcal{E}}{\partial t} \simeq \int dydz \left[\varphi \frac{\partial^2 \varphi}{\partial x \partial t}\right]_{x=-L}^{x=L} \\
&= -\frac{uL_c}{4\pi} \int_{-\infty}^{+\infty} dk_y \; i \; k_y \left[\varphi^*_{k_y}(x)\partial_x \varphi_{k_y}(x) - \varphi_{k_y}(x)\partial_x \varphi^*_{k_y}(x)\right]_{x=-L}^{x=L} \\
&= -\frac{uL_c}{\pi} \int_0^{\infty} dk_y k_y |A_{k_y}|^2 \; , \qquad (41)
\end{aligned}$$

which is independent of L for $L >> x_0$.

Using formula Eq. (36) for A_{k_y} we perform the k_y integral to obtain the vortex decay rate

$$\begin{aligned}
\frac{dE_v}{dt} &= -\frac{uL_c\varphi_m^2}{4\pi} \int_0^{\infty} dk_y \frac{k_y}{\sqrt{k_0^2 + k_y^2}} exp\left(-\frac{4}{3|\alpha|}(k_0^2 + k_y^2)^{3/2}\right) \\
&= -\frac{B}{3b^{1/3}} \int_b^{\infty} dt exp(-t) t^{-2/3} = -\frac{B}{3b^{1/3}} \Gamma(\frac{1}{3}, b) \qquad (42)
\end{aligned}$$

where $B = uL_c\varphi_m^2/4\pi$, $b = 4k_0^3/3|\alpha|$, $t = b(1 + k_y^2/k_0^2)^{3/2}$ and

$$\Gamma(\zeta, \xi) = \int_{\xi}^{\infty} d\tau exp(-\tau)\tau^{\zeta - 1}$$

is the Incomplete Gamma Function[17]. For large ξ, one can write

$$\Gamma(\zeta, \xi) \approx \xi^{\zeta - 1} exp(-\xi)$$

Therefore for small $\alpha << 4k_0^3/3$, *i.e.*, large b, the decay rate of vortex energy is

$$\frac{dE_v}{dt} \approx -\frac{uL_c\varphi_m^2|\alpha|}{16\pi k_0^2} exp(-\frac{4k_0^3}{3|\alpha|}) \; , \qquad (43)$$

valid for $k_0^2 > 0$. Thus the damping is exponentially small provided $k_0^3 > 3\alpha/4$, or in terms of the vortex length scale, $\rho_{s0} << r_0 \sim k_0^{-1} << (4/3\alpha)^{1/3}\rho_{s0} \sim \rho_{s0}/\epsilon^{2/3}$. The damping time

scale τ_L for the decay of the vortex can be estimated by

$$\tau_L = \frac{E_v}{|dE_v/dt|} \approx \frac{2.8\pi^2}{u|\alpha|}(\frac{4}{3} + k_0^2)exp(\frac{4k_0^3}{3|\alpha|}) \ . \tag{44}$$

The theory for the effect of the inhomogeneity in Eqs. (32)-(44) is based on the observation[4] that for strong vortices ($\Omega_E/\omega_k >> 1$ where Ω_E is the rotation frequency in the core of vortex and $\omega_k \simeq k_y u$), the inhomogeneity causes a leakage of wave energy from the vortex core, but does not strongly alter the interior solution. At some stronger level of inhomogeneity the core of the vortex is changed, and non-perturbative solutions exhibiting the effect of inhomogeneity are required.

V. Numerical Vortex Solution in Inhomogenous Plasma

In order to facilitate the numerical solutions of Eq. (5), we first expand the equation according to the ordering in Eq. (24) and consider $\epsilon_t \sim \epsilon$. Keeping only the terms of order ϵ and ϵ^2, we derive from Eq. (5) the reduced dynamical equation

$$\left(\frac{1}{T(x)} - \nabla^2\right)\frac{\partial\varphi}{\partial t} + (v_{d0} + v'_{d0}x - \kappa_T\varphi)\frac{\partial\varphi}{\partial y} - \left[\varphi,\ \nabla^2\varphi\right] = 0 \ , \tag{45}$$

which is valid only when the condition of Eq. (29) is satisfied. In later work we will present numerical solutions of the full Eq. (5) to compare with those presented here.

Rewriting Eq. (45), we get the conservation of mass in the two-dimensional system,

$$\frac{\partial}{\partial t}\left(\frac{\varphi}{T(x)}\right) + \nabla\cdot\left[-\frac{\partial\nabla\varphi}{\partial t} + \left(v_d(x)\varphi - \frac{\kappa_T\varphi^2}{2}\right)\hat{\mathbf{y}} + (\nabla\varphi\times\hat{\mathbf{z}})\nabla^2\varphi\right] = 0 \ . \tag{46}$$

Multiplying Eq. (45) by φ, we can derive the energy conservation law given by Eqs. (37), (38) and (39) in the previous section. The constants are subsequently used to monitor the solutions.

To solve Eq. (45), we use a uniform grid over x and k_y in 85×85 xk_y-space with 3655 complex $\varphi_{x,k_y}(t)$ modes. Since the first term of Eq. (45) depends on x, transforming Eq. (45)

into $k_x k_y$ space would lead to a difficult convolution integral in k_x for the linear problem. Leaving the equation in x space and using the second order centeral difference formula for ∂_x^2, gives a tridiagnal system to solve for each $\partial_t \varphi(x, k_y, t)$. We use the Ahlberg-Nilson-Walsh algorithm for the cyclic tridiagonal systems [18] to reduce the operator $(1/T(x) - \nabla^2)$ as a cyclic tridiagonal matrix and then compute $\partial\varphi/\partial t$ for each mode, in which process the nonlinear convolution terms in Eq. (45) are evaluated by first transforming φ in $k_x k_y$ space to get derivatives of φ, then transforming φ and its derivatives into xy space to calculate the convolutons and, after that, transforming the results back into xk_y space. Finally we use high order Runge-Kutta time stepping and the Fourier Transformation $y \leftrightarrow k_y$ at each time step. The constants of motion defined in Eqs. (37) and (46) are used to monitor the accuracy of the codes. The approximate monopole solution Eq. (26) is taken as the initial condition $\varphi(x, y, t = 0)$. The temperature profile $T(x) = exp(-c_2 x)$ which avoids the negative temperature problem that arises when expanding $T(x)$ as $1 - c_2 x$. For this profile $\kappa_T = c_2 exp(c_2 x)$. Typical simulations average 15 minutes CPU time on the CRAY-II for $\triangle t$=100 r_n/c_s, which is about 10 rotations of the vortex core.

In the first case we used $v'_{d0} = -0.1 v_{d0}$, u=1.1v_{d0} and $c_2 = -0.011$, which give $k_0^2 = (1 - v_{d0}/u) \simeq 0.1$ and $\alpha \simeq (c_2 - v'_{d0}/u) \simeq 0.08$. Therefore α is the same order as k_0^3. We observed the forming of a oscillating tail with significant amplitude and a strong damping process of the monopole vortex. Figure (2) shows the streamline of $\varphi(x, y, t) = const.$ at times tc_s/r_n =0 and 80, and the projections of their crosssections in the x and y directions. The particle density is, from Eq. (28), $n/n_0 \approx exp(\epsilon_n \varphi_m) \approx 1.7$.

In the second case $v'_{d0} = 0.05 v_{d0}$, u=1.1v_{d0} and c_2=0.046, and thus $\alpha \simeq 0.0006$ and $k_0^3 \simeq 0.027$. We can see in Fig. (3) that the amplitude of the oscillatiing tail is so insignificant that the monopole vortex keeps its shape for a long time without much damping. The particle density in this case is $n/n_0 \simeq 0.58$.

Although in the above two cases, we only discussed the anticyclone vortex ($\varphi > 0$) in the

first case, and only the cyclone vortex ($\varphi < 0$) in the second case. In fact, the same results can be obtained for the cyclone vortex in the first case and the anticyclone vortex in the second case, because Eq. (45) possesses the following symmetry relation

$$\varphi(\kappa_T, v'_{d0}; x, y, t) = -\varphi(-\kappa_T, -v'_{d0}; -x, y, t).$$

In Fig. (4), we used same the parameters and initial condition as those in Fig. (3), but dropped the scalar nonlinear term with coefficient κ_T in Eq. (45). The monopole vortex in this case is shown to connect to a radiation wake.

These numerical results support our arguments that when the drift velocity depends on the space variable, the monopole-like vortices can exist in the wavelengh $\sim (\rho_s r_n)^{1/2}$ region. The simulations also verify that the stability of the vortices is affected by the combined effect of temperature and drift velocity gradients and that the vortices are stable or free of damping only when $\alpha << (4/3)k_0^3$.

VI. Summary and Conclusions

We have studied the effect of density and temperature gradients on drift wave vortices, both analytically and numerically. The results show that when the drift wave velocity v_d does not depend on the space variable, localized monopole vortices can not be formed in the long wavelength $\sim (\rho_s r_n)^{1/2}$ region for the choice of F of Eq. (11), no matter what the temperature profile is. When the drift wave velocity is not constant, monopole vortex solutions can be found in the wavelength $\sim \rho_s/\epsilon^{1/2}$ region. However, the important result is that the monopole vortices are not strictly localized monopoles found by many other authors[5,7,8,12]. Although the gradient of the drift velocity is responsible for the formation of the monopole vortices, its existence also causes the formation of the oscillating tails or radiative wakes of drift waves, which connect to the cores of the vortex. The results show that as long as $\alpha \equiv (\kappa_T - v'_{d0}/u) \neq 0$, the wave energy of the vortices leaks out

through the oscillating tails from the vortex cores. The effect of the temperature gradient here is to reduce the energy leakage. The analytic and numerical results also show that only when the combined effect of the temperature and the drift velocity gradients satisfies $\alpha \equiv (\kappa_T - v'_{d0}/u) << (4/3)(1 - v_{d0}/u)^{3/2}$, will the leakage be small and negligible.

Acknowledgments

The authors gratefully acknowledge the aide of V.P. Pavlenko during the course of this investigation and thank B. Scott for his useful suggestions on the numerical simulation. The work was supported by the U.S. Department of Energy contract #DE-FG05-80ET-53088.

References

1. A. Hasegawa and K. Mima, Phys. Fluids **21** 87 (1978); A. Hasegawa, C.G. Maclennan, and Y. Kodama, Phys. Fluids **22**, 2122 (1979).

2. M. Makino, T. Kamimuya, and T. Tanuiti, J. Phys. Soc. Jpn. **50**, 908 (1981).

3. J.D. Meiss and W. Horton, Phys. Fluids **26**, 990 (1983).

4. W. Horton, Phys. Fluids B **1**, 424 (1989).

5. V.I. Petviashvili, Fiz. Plazmy **3**, 270 (1977) [Sov. J. Plasma Phys. **3**, 150 (1977)].

6. X. Su, W. Horton, P.J. Morrison, and V.P. Pavlenko, "Effect of Scalar Nonlinearity on the Dipole Vortex Solution", U. of Texas at Austin, IFSR# 328, (1988).

7. V.P. Lakhin, A.B. Mikhailovskii and O.G. Onishchenko, Phys. Lett. A **119**, 348 (1987), and Plasma Physics and Controlled Fuison **30**, 457 (1988).

8. S. Horihata and M. Sato, J. Phys. Soc. Jpn. **56**, 2611 (1987).

9. J. Nycander, Phys. Fluids B **1**, (9) 1788 (1989).

10. E.W. Laedke and K.H. Spatschek, Phys. Fluids **31**, 1492 (1988).

11. M.V. Nezlin, Sov. Phys. Usp. **29**, 807 (1986) [Usp. Fiz. Nauk **150**, 3 (1986)].

12. K.H. Spatschek, E.W. Laedlke, Chr. Marquardt, S. Musher, H. Wenk, Phys. Rev. Lett. **64**, 3027 (1990).

13. W. Horton, T. Tajima, and T. Kaminura, Phys. Fluids **30**, 3485 (1987).

14. R. Z. Sagdeev, V. D. Shapiro, and V. I. Shevchenko, Sov. Astron. Lett. **7**, 279 (1981).

15. V.I. Petviashivili, Pisma Zh. Eksp. Teor. Fiz. **32**, 632 (1980) [JETP Lett. **32**, 619 (1980)].

16. W. Magnus and F. Oberhettinger "Formulas and Theorems for the Special Functions of Mathematical Physics", (Chelsea, New York, 1949) (Translated from the German by J. Wermer) pp. 118.

17. M. Aramowitz and I.A. Stegun "Handbook of Mathematical Functions with Formulas, Graphs, and Mathematical Tables" (Dover, New York, 1965) pp. 260-263.

18. C. Temperton, J. Comp. Phys. **19**, 317 (1975).

Figure Captions

1. (a) Contour plot of the electrostatic potential $\varphi(x,y,t)$ in Eq. (45). The dipole vortex (solution of the H-M equation) is taken as initial condition in Eq. (45) with $T(x) = exp(-c_2 x)$, $c_2 = 0.046$, $u = 1.1$, $r_0 = 6.0$, and $v'_{d0} = 0.05$. The solid lines represent positive values of potential φ, and the dashed lines are negative values. (b) The dipole vortex is first split into two monopoles, cyclone ($\varphi < 0$) and anticyclone ($\varphi > 0$). (c) Finally only the cyclone survives.

2. Contour plot of the electrostatic potential $\varphi(x,y,t)$ in Eq. (45) with $T(x) = exp(-c_2 x)$, $c_2 = -0.011$, $v'_{d0} = -0.1 v_{d0}$, and $u = 1.1 v_{d0}$ so that $k_0^3/\alpha \simeq 0.34$. The contour interval $\triangle\varphi$=0.8. (a) The initial condition is a monopole defined by Eq. (26). (b) At $t = 40 r_n/c_s$, the monopole vortex core is coupling to an oscillating tail, *i.e.* a radiative wake of drift waves. (c) At $t = 60 r_n/c_s$, the monopole vortex has been strongly distorted and the amplitude has been significantly decreased from $5.28(T_0/e)(\rho_{s0}/r_n)$ at beginning to $3(T_0/e)(\rho_{s0}/r_n)$, due to the strong damping.

3. Same as above with $c_2 = 0.046$, $v'_{d0} = 0.05 v_{d0}$, and $u = 1.1 v_{d0}$, which give $k_0^3/\alpha \sim 45$, (a) the contours of $\varphi(x,y,t)$ at $t = 0$ show the initial state given by Eq. (26). (b) At $t = 40 r_n/c_s$, the amplitude of the oscillating tail is too small to be noticed. (c) and (d) At $t = 80 r_n/c_s$ and $100 r_n/c_s$, the monopole vortex still keeps its shape with very slight distortion in the exterior region and the amplitude still has no significant change.

4. The parameters and the initial condition are same as those in Fig. (3), but the scalar nonlinear term with coefficient κ_T in Eq. (45) is dropped. The monopole vortex in this case is shown to connect to a radiation wake.

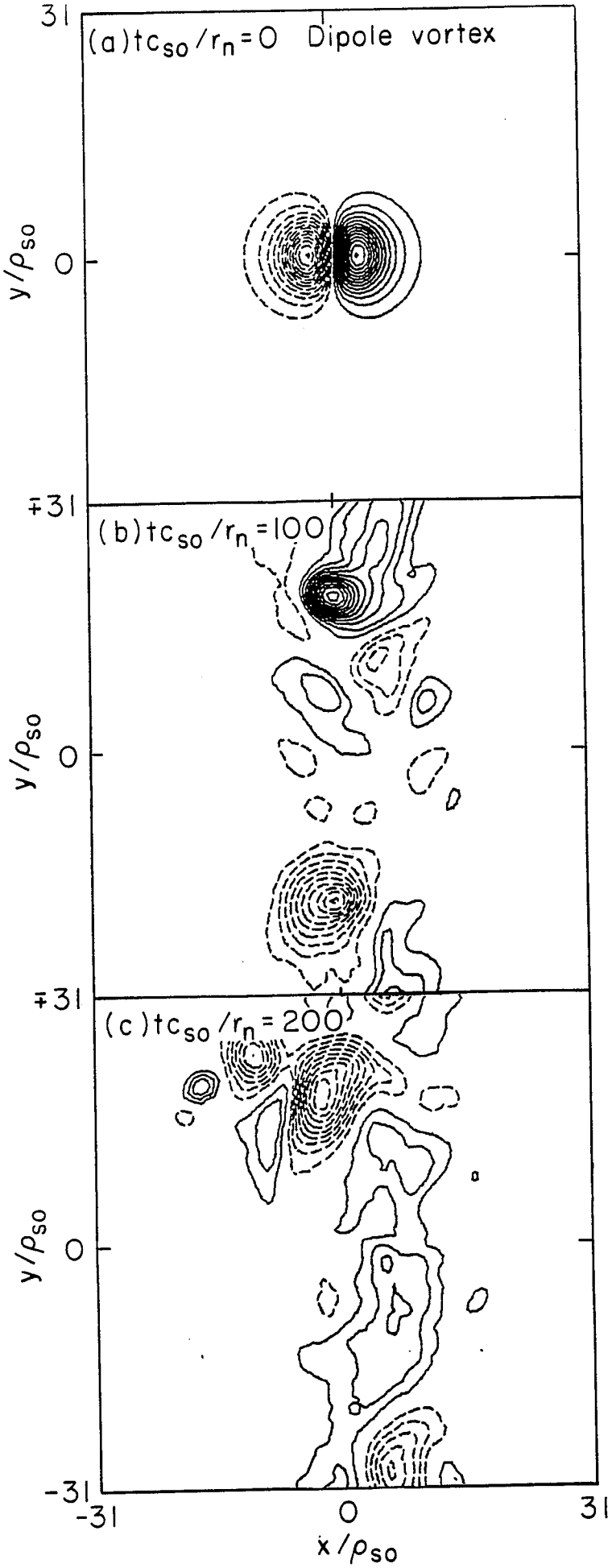
(a) $tc_{so}/r_n = 0$ Dipole vortex
(b) $tc_{so}/r_n = 100$
(c) $tc_{so}/r_n = 200$
31
0
-31
y/ρ_{so}
x/ρ_{so}

Fig. 1

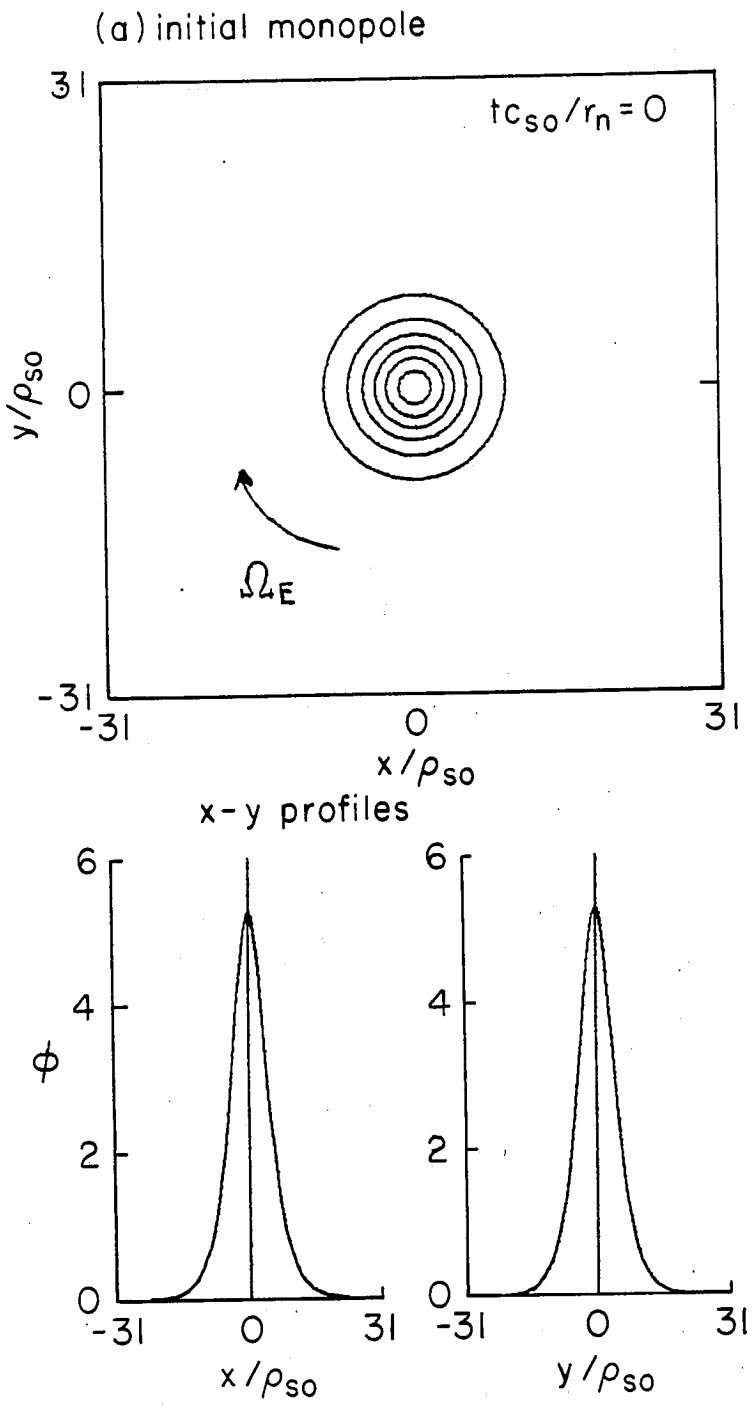
(a) initial monopole
$tc_{so}/r_n = 0$
31
0
-31
y/ρ_{so}
Ω_E
-31
0
31
x/ρ_{so}
x-y profiles
6
4
2
0
ϕ
-31
0
31
x/ρ_{so}
y/ρ_{so}

Fig. 2 (a)

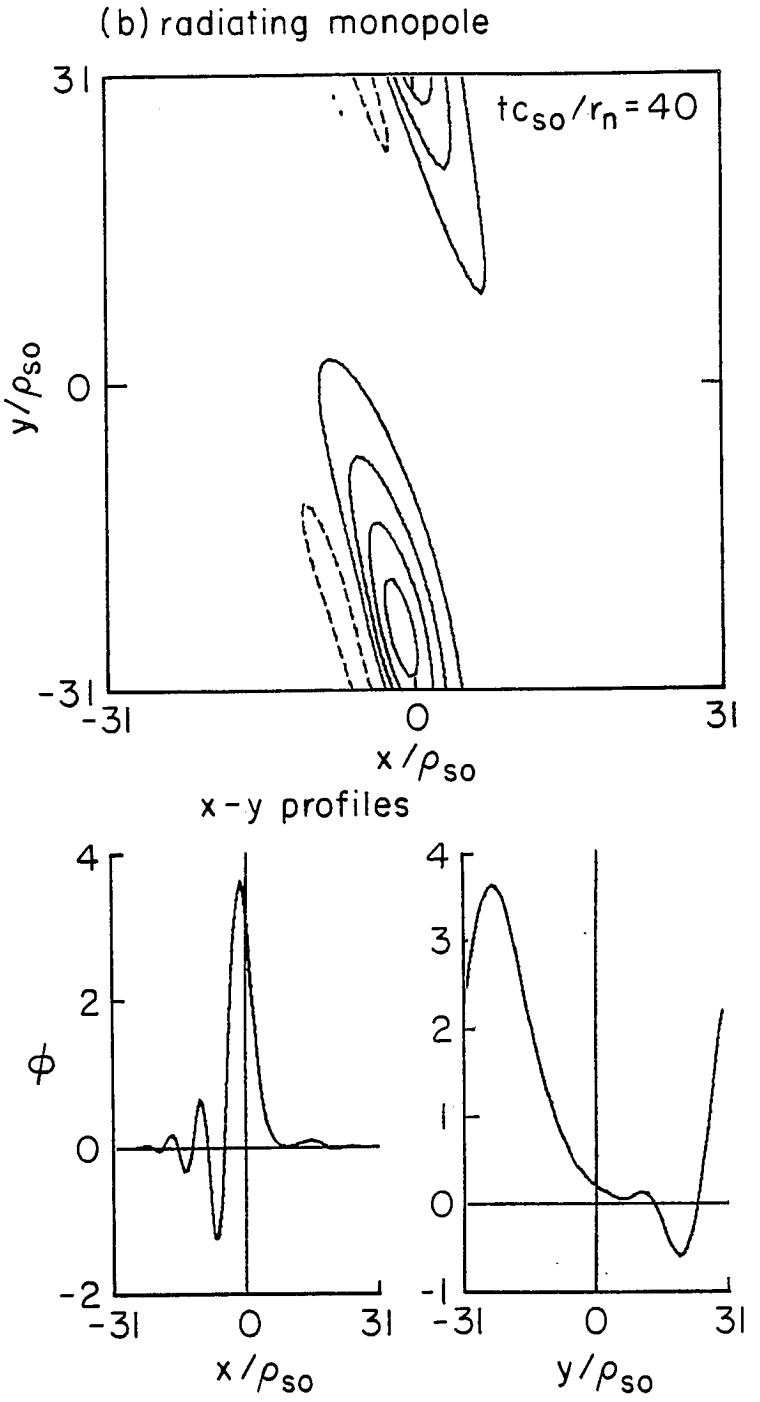
(b) radiating monopole
$tc_{so}/r_n = 40$
31
0
-31
y/ρ_{so}
-31
0
31
x/ρ_{so}
x-y profiles
4
2
0
-2
ϕ
-31
0
31
x/ρ_{so}
4
3
2
1
0
-1
-31
0
31
y/ρ_{so}

Fig. 2(b)

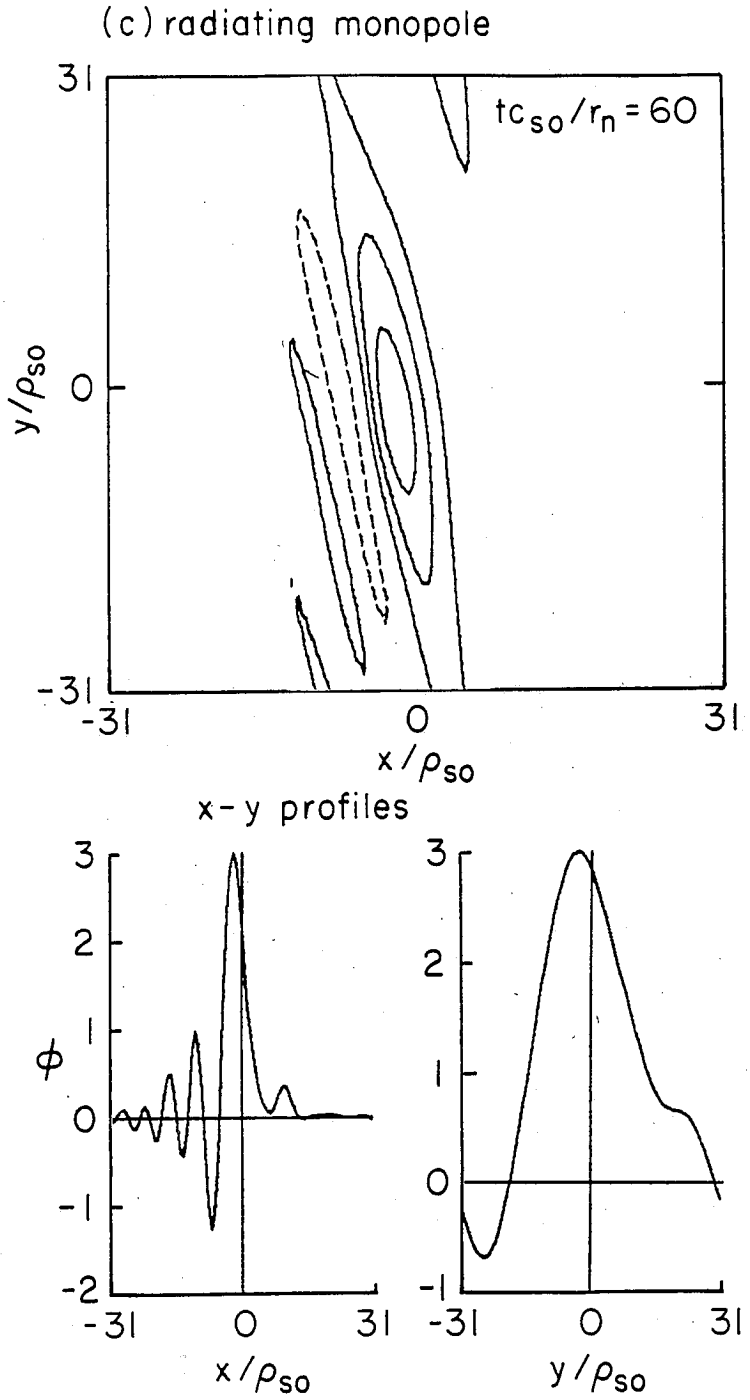
(c) radiating monopole
$tc_{so}/r_n = 60$
31
0
-31
y/ρ_{so}
-31
0
31
x/ρ_{so}
x-y profiles
3
2
1
0
-1
-2
ϕ
-31
0
31
x/ρ_{so}
3
2
1
0
-1
-31
0
31
y/ρ_{so}

Fig. 2(c)

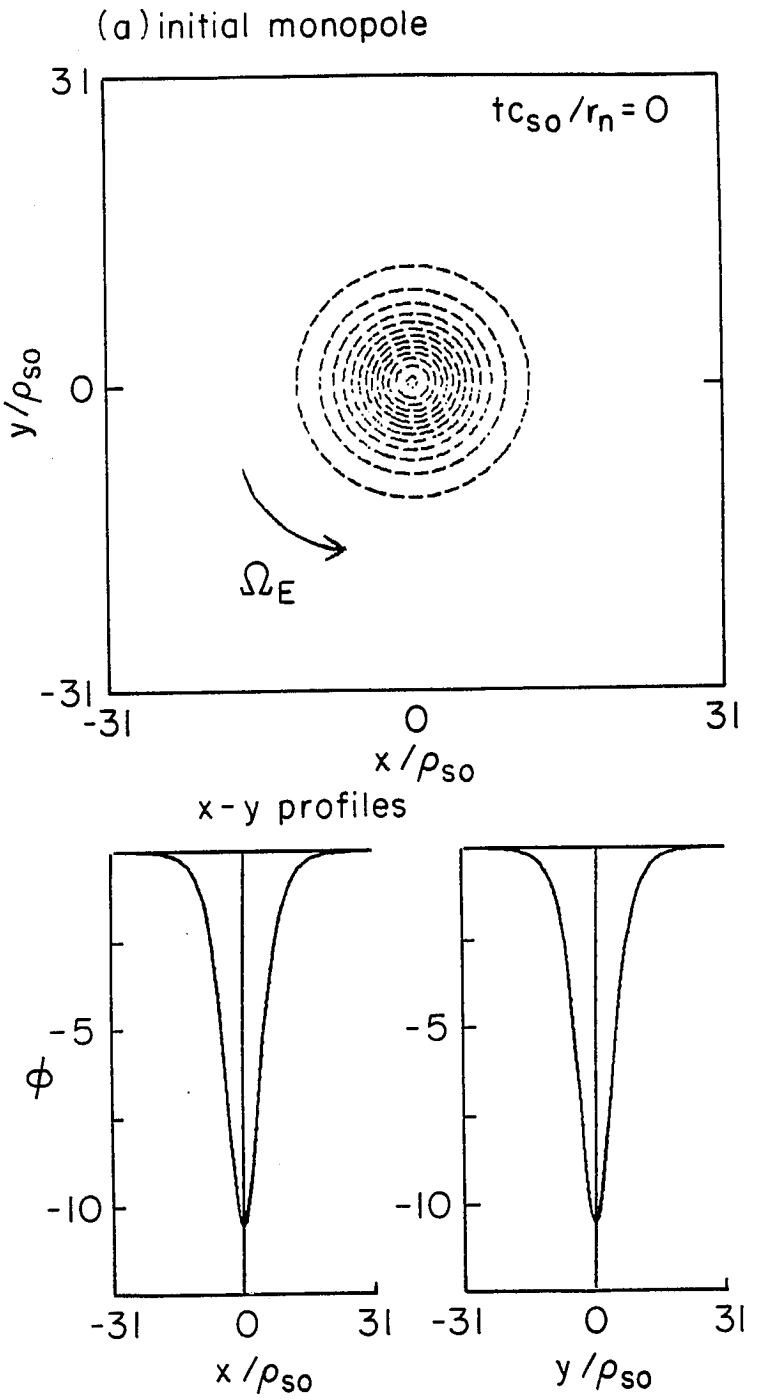
(a) initial monopole
31
$tc_{so}/r_n = 0$
y/ρ_{so}
0
Ω_E
-31
-31
0
31
x/ρ_{so}
x - y profiles
ϕ
-5
-10
-31
0
31
x/ρ_{so}
-5
-10
-31
0
31
y/ρ_{so}

Fig. 3(a)

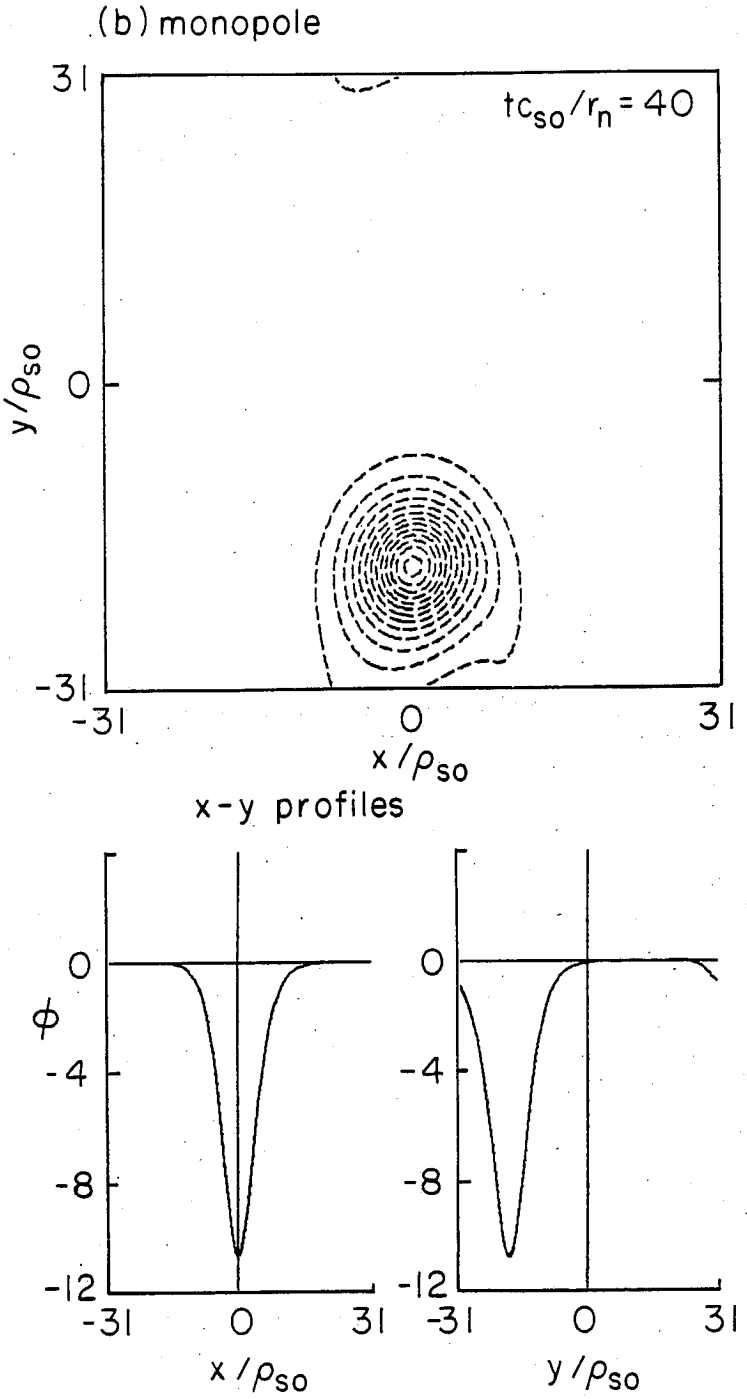
(b) monopole
$tc_{so}/r_n = 40$
31
0
-31
y/ρ_{so}
-31
0
31
x/ρ_{so}
x-y profiles
0
-4
-8
-12
ϕ
-31
0
31
x/ρ_{so}
y/ρ_{so}

Fig. 3(b)

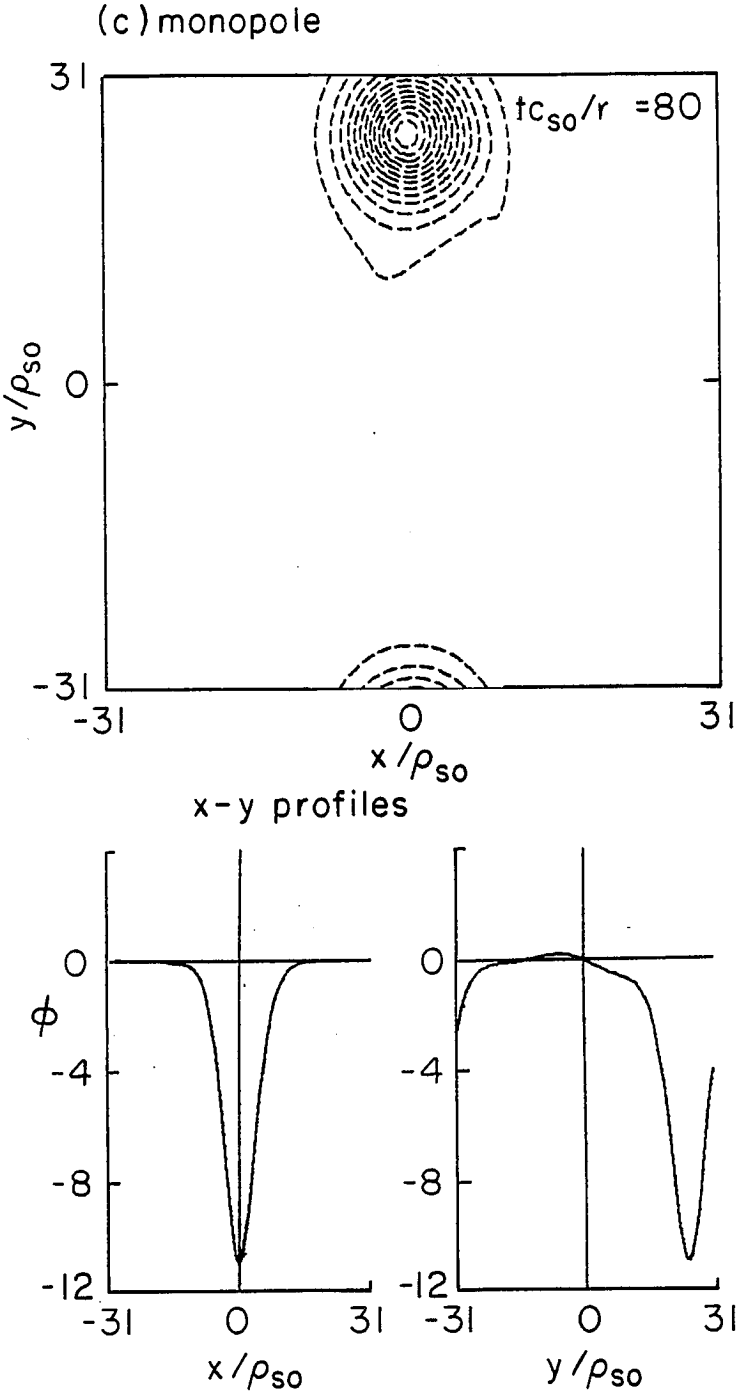
(c) monopole
tc_{so}/r =80
31
0
-31
y/ρ_{so}
-31
0
31
x/ρ_{so}
x-y profiles
0
-4
-8
-12
ϕ
-31
0
31
x/ρ_{so}
0
-4
-8
-12
-31
0
31
y/ρ_{so}

Fig. 3(c)

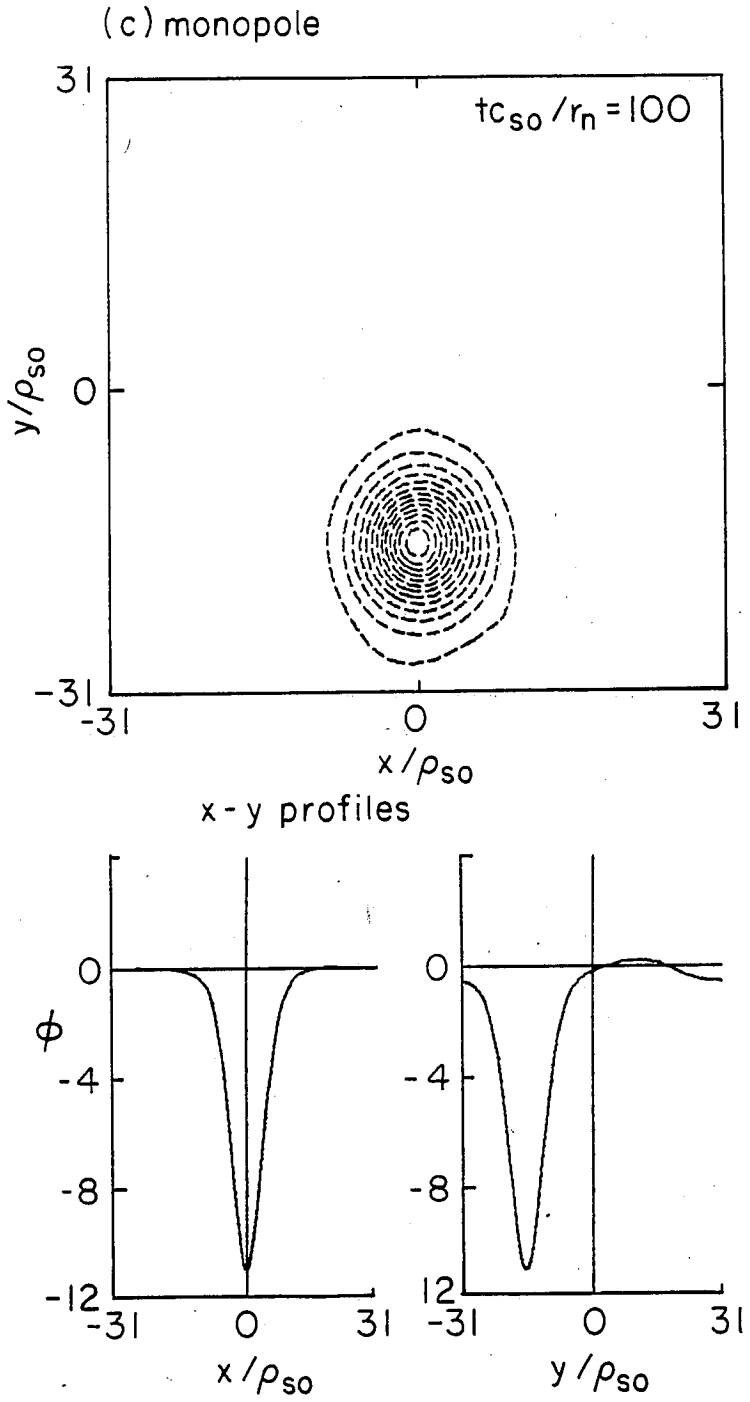
(c) monopole
$tc_{so}/r_n = 100$
31
0
-31
y/ρ_{so}
-31
0
31
x/ρ_{so}
x - y profiles
0
ϕ
-4
-8
-12
-31
0
31
x/ρ_{so}
0
-4
-8
12
-31
0
31
y/ρ_{so}

Fig. 3(d)

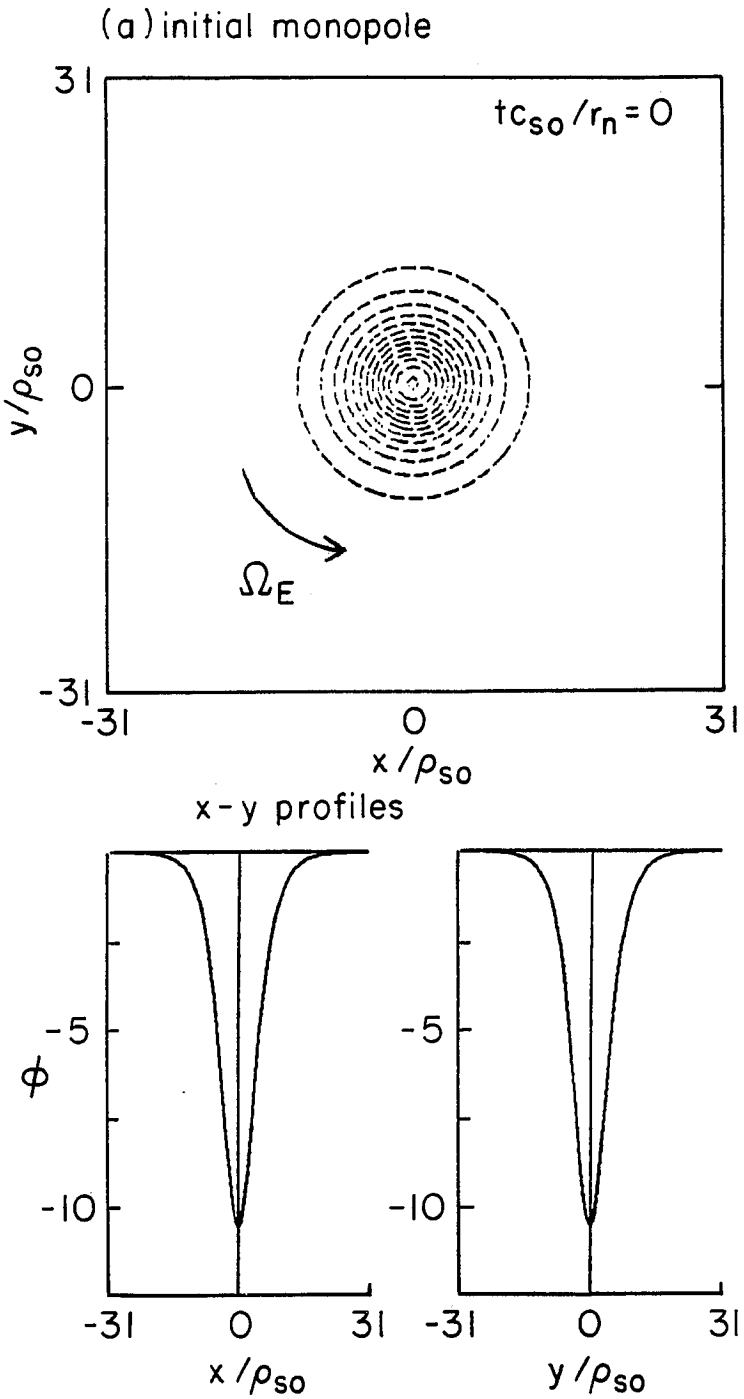
(a) initial monopole
31
$tc_{so}/r_n = 0$
y/ρ_{so}
0
Ω_E
-31
-31
0
31
x/ρ_{so}
x-y profiles
ϕ
-5
-10
-31
0
31
x/ρ_{so}
-5
-10
-31
0
31
y/ρ_{so}

Fig. 4(a)

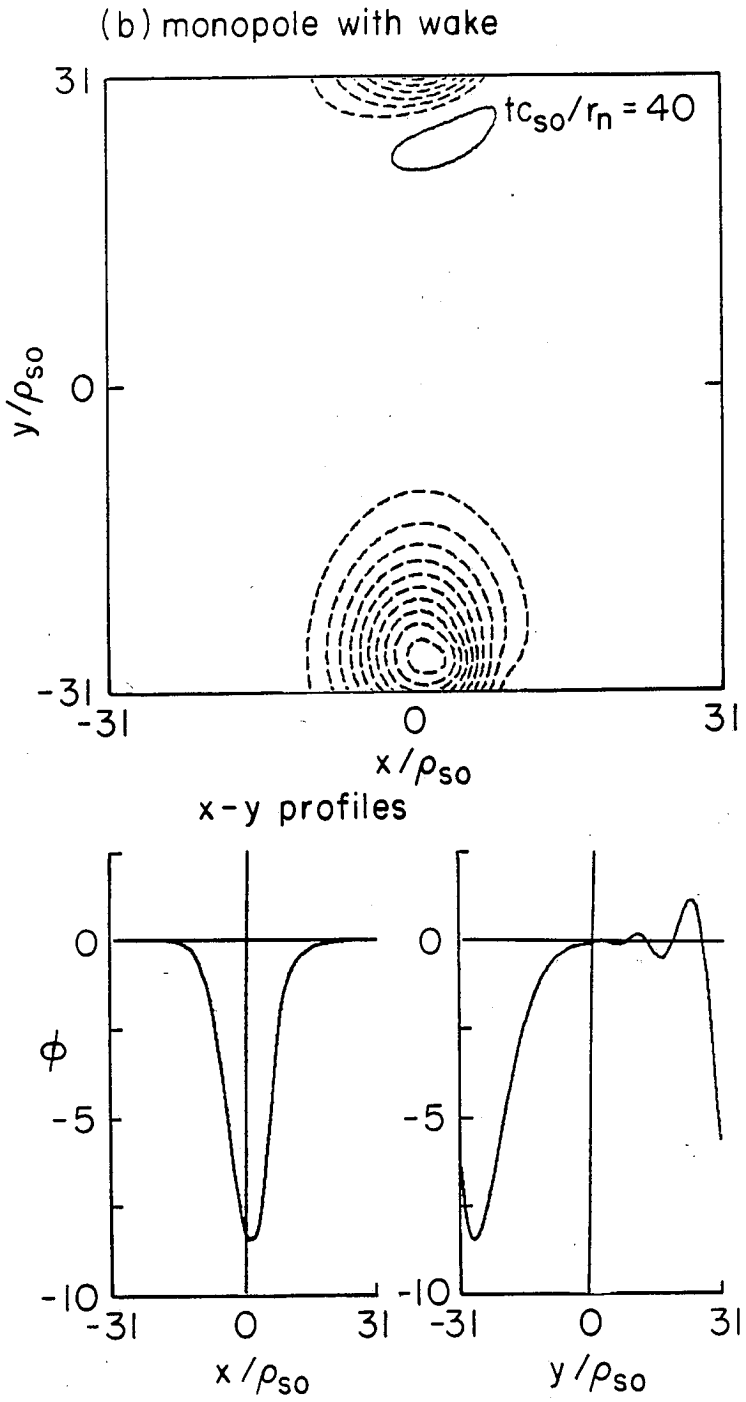
(b) monopole with wake
31
$tc_{so}/r_n = 40$
y/ρ_{so}
0
-31
-31
0
31
x/ρ_{so}
x-y profiles
0
ϕ
-5
-10
-31
0
31
x/ρ_{so}
0
-5
-10
-31
0
31
y/ρ_{so}

Fig. 4(b)

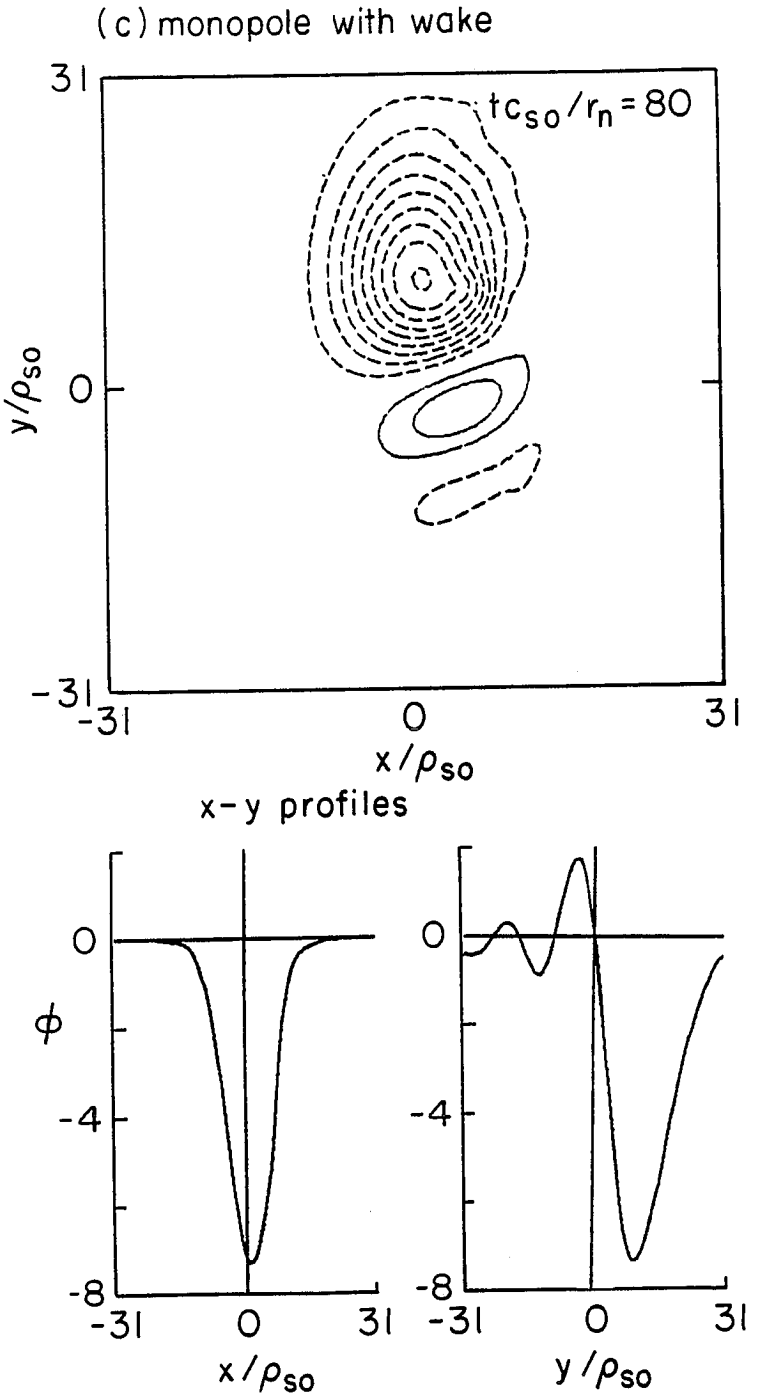
(c) monopole with wake
31
$tc_{so}/r_n = 80$
y/ρ_{so}
0
-31
-31
0
31
x/ρ_{so}
x-y profiles
0
ϕ
-4
-8
-31
0
31
x/ρ_{so}
0
-4
-8
-31
0
31
y/ρ_{so}

Fig. 4(c)